ICMIEE20-KN05

Bioinspired Electrospun Nanocomposites: An Emerging Technology of Atmospheric Fog Water Generator

Md. Nizam Uddin, Balakrishnan Subeshan, Muhammad Mustafizur Rahman[*]*, Ramazan Asmatulu*
Department of Mechanical Engineering, Wichita State University, 1845 Fairmount Street, Wichita, KS-67260-0133, USA

ABSTRACT

Nature-inspired fog harvesting is a promising technology aimed at acquiring freshwater from the atmosphere. However, the design of nature-inspired surfaces with unique characteristics for this specific application provides a paradigm shift in the development of the new engineering surfaces. Efficient fog collecting nanofibers were designed with the inspiration of fog-harvesting capability of Stenocara beetles in the Namib Desert. Several available polymers such as polyacrylonitrile (PAN), polymethyl methacrylate (PMMA), recycled expanded polystyrene (EPS) foam with various proportions of titanium dioxide (TiO_2) nanoparticles, and aluminum (Al) microparticles were spun into superhydrophobic-hydrophilic nanocomposite fibers using the facile electrospinning technique. The fiber morphology, wetting characteristics, and fog-harvesting capacity of the nanocomposites were investigated. The as-prepared PAN/PMMA and EPS nanocomposites having 10% inclusion of combined micro-and nanoparticles exhibit superhydrophobic characteristics i.e. a water contact angle of 154.8° and 152.03° respectively. The experimental tests of PAN/PMMA and EPS nanocomposites reveal the daily freshwater productivity of more than 1.49 liter/m^2 and 1.35 liter/m^2 of nanocomposites. The cost of materials formaking such nanocomposites to supply estimated daily water consumption for a household with 2 members (i.e., 6 liters) is only US$2.67 (EPS nanocomposite) and US$4.97 (PAN/PMMA nanocomposite). These nanocomposites harvest fog water without any additional energy input or any large infrastructure thus, it's cheap and affordable. This technology offers a novel and very cost effective tool for the production of freshwater in arid areas.

Keywords: Electrospinning, carbonization, superhydrophobicity, fog water generator.

1. Introduction

The global water shortage problem has given rise to the evolution of water-capturing technology since the 20th century, particularly in arid and semi-arid countries. However, atmospheric fog can account for a considerable number of freshwater sources. The atmosphere holds 37.5 million billion gallons of water in the invisible vapor phase [1]. The United Nations Convention to Combat Desertification reports that by 2025 about 2.4 billion people will suffer from water scarcity [2]. Hence, engineers and scientists are confronted with discovering economically suitable and applicable water resources to solve the problem. In some countries, possible systems include rain and groundwater harvesting. The cloud seeding is also used in some locations. These systems typically produce clean water for drinking, agriculture, medical, and other purposes [3]. Harvesting fog water with high efficiency is an attractive proposal to relieve the risk of water shortage [4].

In nature, many animals and plants have special surface wetting characteristics designed with a combination of micro-and nanoscale structures [5-11]. For example, the Stenocara beetle harvests water instantly from the fog and mist. This beetle's carapace has a combination of hydrophilic bumps and a hydrophobic surface. These hydrophilic bumps capture the fog droplet, carried by wind and coalescence, and then the hydrophobic surface directs the water straight to the beetle's mouth [12]. Cribellate spiders utilize silk with spindle-knots and a joint structure that allows wettability and curvature gradients to capture water from the atmosphere [5]. Only a few studies have considered the fabrication of superhydrophobic polymeric nanocomposite fibers for water harvesting using nanotechnology [13]. Wang et al. fabricated the hydrophilic-superhydrophobic surface for efficient fog collection in 2015. The hybrid surface is produced with superhydrophobic structure transformed metal-based gauze bonded to the surface of the hydrophilic polystyrene (PS) flat sheet. The hydrophilic-superhydrophobic designed hybrid surface obtained a high collection capacity of 159 mg/cm^2/h [14].

In another study, fourteen polyethylene terephthalate (PET) fibers with individual cross-sections and surface structures such as microgrooves were fabricated, and fog collection efficiency was measured. It was witnessed that micro-grooved fiber surfaces rise depositing efficiency and enhance drainage efficiency [15]. Almasian et al. fabricated fluorinated superhydrophobic PAN nanofibers for studying their fog-harvesting properties. The fabrication method was optimized by variable temperature, time, and quantity of fluoroamine compound. Fabricated PAN nanofibers showed a water contact angle of 159° and a low surface energy of 17.1 mN/m. The highest fog-harvesting capacity of 335 mg/cm^2.hr was attained when the nanofibers were dried for 3 hr at 95°C, and the quantity of fluoroamine compound was 8% (w/w) in the process [16]. Even though plenty of methods have been established to resemble the structure on Stenocara beetles' back for water-harvesting, however, places, where peoples are suffering for water, is poverty-stricken and underdeveloped regions, where materials and manufacturing services are insufficient [17-18]. Hence, simple fabrication, mass production, and handling of fog water harvesting materials remain as issues to be solved for wide application of this new technology. Our study

* Corresponding author. Tel.: +1-813-751-7190
E-mail addresses: muhammad.rahman@wichita.edu

focuses on fabricating superhydrophobic-hydrophilic nanocomposite fibers via electrospinning using two types of polymers, namely PAN/PMMA and waste EPS foam with the introduction of TiO_2 nanoparticles and Al microparticles. Thesurface wetting characteristics, morphology of fibers, and fog water harvesting performance were studied.

2. Experimental Setup

2.1 Materials

PAN (molecular weight, Mw 150,000 g/mole, Tg 95°C) and PMMA (Mw 120,000 g/mole, Tg 99.0°C) were purchased from Sigma-Aldrich (St. Louis, MO, USA). The waste EPS was collected from the packaging of laboratory chemicals. TiO_2 nanoparticles of average particle size of 40 nm (anatase, 99.5%) and Al microparticles (99.7%, 10 µm) were both purchased from U.S. Research Nanomaterials Inc., TX, USA. All materials used in this study were original without any modifications to the supplier specifications.

2.2 Fabrication of Polymer Nanocomposite

The nanocomposite fibers using two types of polymers were fabricated using the facile electrospinning method. Both types of polymers were dissolved in DMF at a ratio of 80:20 at 45°C and stirred for 2 h to obtain a homogeneous polymeric solution. The ratio of PAN and PMMA was 25:75 percent by weight. Different concentrations of micro-and nanoparticles were used (0, 2.5, 5, and 10 wt%) to fabricate the nanocomposite fibers which were added into the polymer solution and stirred for another 2 h, followed by 20 min of probe sonication to produce a homogeneous polymer solution. The prepared solution was electrospun and then dried for 24 h in an open atmosphere. The electrospinning was conducted at 25 kV, and a feed rate of 1 ml/h and the distance between the tip and collector was 25 cm. The fabricated nanocomposite fibers were then stabilized and carbonized at 250°C and 850°C for 1 h in an oxygen and argon environment respectively to separate the entire remnant solvent and retained moisture. The electrospinning procedure limits were held steady for each type of polymers produced in the study. Fig. 1 demonstrates a step-by-step demonstration of the fabrication process of electrospun nanocomposite fibers.

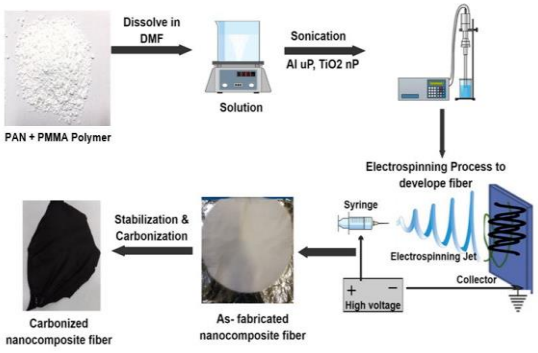

Fig. 1 Illustration of the fabrication process of electrospun nanocomposite fibers.

2.3 Characterization of Nanocomposite Fibers

The wetting characteristics of the nanocomposites were measured with a water contact angle goniometer (KSV Instruments Ltd., Model #CAM 100). A scanning electron microscopy (SEM) (FEI Nova Nano SEM 450) was used to study the morphology of the nanocomposites. The surface roughness was measured by a Mitsutoyo 178-561-02A Surftest SJ-210 Surface Roughness Tester. Over a range of 3500−500 cm^{-1}, the surface chemistry of the nanocomposite fibers was achieved by Fourier-transform infrared spectroscopy (FTIR) (Thermo Scientific™ Nicolet™ iN10 infrared microscope).

3. Results and Discussion

3.1 Characteristics of Nanocomposite

Fig. 2 displays the FTIR spectra of the carbonized PAN/PMMA nanocomposite. The PAN molecule is a sequential arrangement of methyl (CH_3) and nitrile (C≡N) groups [19]. However, when the carbonization process occurs at a high temperature of 850°C, entire volatile compounds are burnt out, which leaves only carbon and hydrogen molecules in the carbon fiber structure. The peak intensities at 987 and 1450 cm^{-1} are given to the aliphatic CH group vibration of various modes in CH_2 and CH correspondingly in the spectrum of untreated fiber. The bands corresponding to 1150 and 1720 cm^{-1} are because of C-O and C=O stretching, and the bands corresponding to 1240 and 2360 cm^{-1} are C-N and C≡N stretching. The absorption peaks of C-O and C=O groups deteriorate slowly with the accumulation of Al microparticles and TiO_2 nanoparticles. Most significantly, all the strong peaks vanished after carbonization. The intensity bands at all peaks vanished, compared to the untreated PAN/ PMMA fibers spectrum.

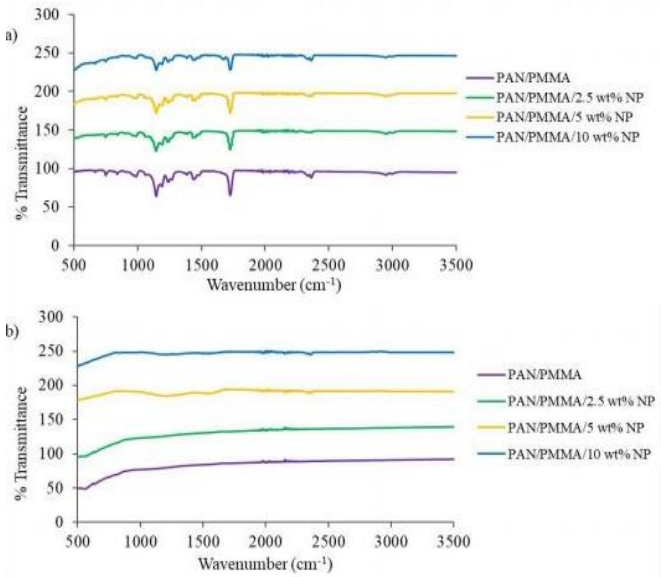

Fig. 2 FTIR spectra of nanocomposite fibers: (a) as prepared and (b) after carbonization.

The average roughness of the as-prepared PAN/PMMA nanocomposite fibers showed 0.34±0.02 µm, and it was influenced substantially due to the

introduction of micro and nanomaterials. For 2.5, 5, and 10 wt.% inclusions of micro and nanomaterials, the average roughness of the PAN/PMMA nanocomposite fiber were 0.49±0.03, 0.94±0.05, and 1.77±0.04 µm respectively. However, EPS nanocomposite with 0 wt% micro and nanomaterials showed the roughness of 0.78±0.03 µm. For 5, 10, and 15 wt% inclusions of micro and nanomaterials, the average roughness of the EPS nanocomposite was 1.35±0.02, 1.81±0.04, and 2.55±0.05 µm, respectively, as shown in Table 1. Various chemical stimulations, including degradation, cross-linking, and cyclization, can happen due to the high-temperature heat treatment of the PAN/PMMA nanocomposite. The mechanism of the process is based on the polymer and type, inclusion percentage, and heating rate [20].

Table 1 The average roughness of various nanocomposites.

Nanocomposite	Average Roughness (Ra, µm)	Nanocomposite	Average Roughness (Ra, µm)
PAN/PMMA	0.34±0.02	EPS	0.78±0.03
PAN/PMMA/2.5 wt% NP	0.49±0.03	EPS/5 wt% NP	1.35±0.02
PAN/PMMA/5 wt% NP	0.94±0.05	EPS/10 wt% NP	1.81±0.04
PAN/PMMA/10 wt% NP	1.77±0.04	EPS/15 wt% NP	2.55±0.05

Fig. 3 presents the SEM images of the PAN/PMMA nanocomposite. As shown in Fig. 3(a), the fibers were noticed significantly fewer beading structures with uniform diameters and smooth surfaces. Fig. 3**Error! Reference source not found.**(c) illustrates the nanocomposite fabricated with an inclusion of 10 wt% of Al and TiO_2 nanoparticles. As the nanoparticle reinforcement increases, the beading and agglomeration of the structure increase, and rough surfaces were produced. Viscosity, conductivity, elasticity, and surface tension of the solution significantly impact the transformation of the polymer solution into nanocomposite.

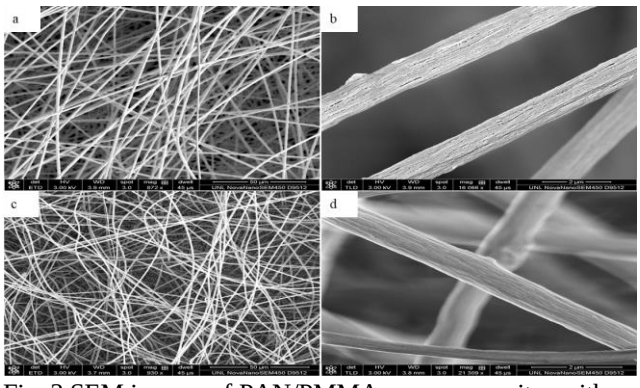

Fig. 3 SEM images of PAN/PMMA nanocomposites with micro and nanomaterials reinforcement at low and high magnification; (a, b) 0 wt% NP and (c, d) 10 wt% NP.

3.2 Wetting Characteristics of Nanocomposite

The average water contact angle of carbonized PAN/PMMA nanocomposite without any inclusion of nanoparticles was 130.88°, and with 10wt% nanoparticles was 154.8°. The maximum average water contact angle of 152.03° was noted for EPS nanocomposite with 10 wt% nanoparticle inclusions. Consequently, the carbonized nanocomposite with 10 wt% inclusions of nano- and microparticles reveal the superhydrophobic property. The water contact angle of the different nanocomposites is summarized in Table 2.

Table 2 The water contact angle of various nanocomposites with Al microparticles and TiO_2 nanoparticles.

Nanocomposite	Water contact angle (º)	Nanocomposite	Water contact angle (º)
PAN/PMMA	130.88±2.43	EPS	116.29±2.75
PAN/PMMA+2.5 wt.% NP	141.62±1.97	EPS/5 wt.% NP	131.99±2.34
PAN/PMMA+5 wt.% NP	149.73±1.34	EPS/10 wt.% NP	152.03±3.16
PAN/PMMA+10 wt.% NP	154.80±3.02	EPS/15 wt.% NP	143.60±2.64

The formation of a ladder-like structure of PAN was developed while stabilizing the nanocomposite at 280°C in an oxygen environment. The primary purpose of the stabilization process during the fabrication is to chemically, physically, and thermally stabilize the nanocomposite fibers, which is a significant factor for superhydrophobicity. Moreover, the nanocomposite is modified from thermoplastic to thermosetting during the stabilization process, which decreases the diameter and changes the color. However, in the carbonization process, the nanocomposite fibers heated at 850°C in an argon environment led to the transformation of nanocomposite fibers into carbon fibers. During this process, PMMA is burned out, leaving porous fibers, and releases the radicals which adhered to the primary chain of the nanocomposite fiber to eliminate the polarity. The surface roughness and porosity generate a noticeable heterogeneous wettability in which the air is entrapped by water in the surface cavities [21-22], which provides less contact area between the water and the solid substrate while improving the contact area between the water and the air, which leads to an increment of wettability of the surface.

3.3 Fog Harvesting Performance of Nanocomposite

The prominent mechanisms that affect fog-harvesting efficiency include capturing, collecting, and transporting. In the capturing phase, the fabricated surface must capture the tiny fog water droplets moving with the flowing air [23]. The harvesting efficiency is subject to the airflow velocity and hydrophilicity of the fabricated surfaces [24]. The collecting phase is vital for a fabricated surface to achieve high efficiency, which can

reduce due to evaporation of fog water droplets in massive airflow. Lastly, in the transporting phase, the fog water droplets roll off the fabricated surface as they grow large enough to break out. The surface area along with the hydrophobicity with the tilted angle significantly influence this phase. All these three phases should be fast enough to reduce evaporation and improve harvesting efficiency. In this study, the fog harvesting performance of PAN/PMMA and EPS nanocomposites were tested by using a tabletop unit. A conventional ultrasonic humidifier was utilized to generate the artificial fog. The humidifier operated with a fog flow velocity of 330 ml/h. The fog collection performance of the nanocomposites were experimented under the temperature and humidity maintained at 19±2°C and 68±3%, respectively. The nanocomposite was located vertically intersecting the fog flow direction. The harvested water by the nanocomposite was collected using a beaker and recorded every 20 min for 60 min. The results of the fog harvesting capacity of two different nanocomposites are presented in Table 3. The nanocomposites with 10 wt% of micro-and nanoparticles exhibited greatest water collecting performance.

Table 3 The fog harvesting capacity of various nanocomposites.

Nanocomposite	Fog harvesting capacity ($gm/cm^2/h$)	Nanocomposite	Fog harvesting capacity ($gm/cm^2/h$)
PAN/PMMA	0.258±0.021	EPS	0.236±0.026
PAN/PMMA/2.5 wt% NP	0.411±0.018	EPS/5 wt% NP	0.468±0.016
PAN/PMMA/5 wt% NP	0.507±0.027	EPS/10 wt% NP	0.561±0.033
PAN/PMMA/10 wt% NP	0.621±0.023	EPS/15 wt% NP	0.387±0.019

The PAN/PMMA nanocomposite without any inclusion of nanoparticles revealed a fog harvesting capacity of 0.258 $gm/cm^2/h$. The highest fog harvesting capacity among all four different PAN/PMMA nanocomposite was 0.621 $gm/cm^2/h$, which is PAN/PMMA with 10 wt% micro-and nanoparticles sample. The EPS nanocomposite without any inclusion of nanoparticles also exhibited the fog harvesting capacity of 0.236 $gm/cm^2/h$, whereas, with the introduction of 5 and 10 wt % micro-and nanoparticles, the fog harvesting capacities rise to 0.468 and 0.561 $gm/cm^2/h$ respectively.

The hydrophilic characteristics of TiO_2 nanoparticles and Al microparticles ameliorate the fog harvesting performance substantially when combined with a superhydrophobic domain. The inclusions of TiO_2 nanoparticles and Al microparticles enhance the water coalescence and condensation process on those surfaces with superhydrophobic domains. The superhydrophobic-hydrophilic hybrid surface validates the superior fog harvesting capacity. Furthermore, the tiny fog water droplets that are captured on the hydrophilic sections typically move toward the hydrophobic sections due to the wettability properties [25]. The collective outcome of the hydrophobic surface with several hydrophilic sites dominate the fog harvesting capacity of the nanocomposite. An efficient fog harvesting nanocomposite must have enough hydrophilic sites to capture and collect the fog water droplets. Accordingly, the nanocomposite with the inclusion of micro-and nanoparticles enhances the surface water droplet coalescence and drainage, which are two challenging progressions in fog harvesting.

4. Conclusions

We developed a simple and affordable fabrication method of superhydrophobic-hydrophilic nanocomposite from PAN/PMMA and waste EPS that offers greater fog harvesting performance. The carbonized PAN/PMMA nanocomposite with 10 wt% nanoparticles inclusion shows superhydrophobic characteristics (water contact angle 154.8°) and daily water productivity greater than 1.49 $liter/m^2$ of the nanocomposite. Similarly, the EPS nanocomposites with 10 wt% nanoparticles inclusion also show superhydrophobic characteristics (water contact angle 152.03°) and daily water productivity of more than 1.35 $liter/m^2$. It is estimated that the materials cost of producing EPS and PAN/PMMA nanocomposites to supply minimum daily water consumption for a household of 2 members is only US$2.67 and US$4.97 respectively. Due to higher fog harvesting capacity and usage durability, the established technology has enormous practical value in large-scale applications. The experimental results show that uniform diameter fibers were produced. It is more reliable to conclude that this technology has potential applications to harvest fog water on a large scale in water-deficient countries.

References

1. Onda, K., Lobuglio, J. & Bartram, J, Global access to safe water: Accounting for water quality and the resulting impact on MDG progress, International Journal of Environmental Research and Public Health, vol. 9, pp. 880–894, 2012.
2. Dooley, E. E., United nations convention to combat desertification. *Environmental Health Perspectives*, vol. 110, 2002. https://www.unccd.int/Sites/Default/Files/Documents/12112014_Invisible%0AFrontline_ENG.Pdf.
3. Uddin, M. N., Alamir, M., Muppalla, H., Rahman, M. M. & Asmatulu, R, Nanomembranes for Sustainable Fresh Water Production, in The 5th *International Conference on Mechanical, Industrial and Energy Engineering* pp. 23–24, 2018.
4. Qadir, M., Jiménez, G. C., Farnum, R. L., Dodson, L. L. & Smakhtin, V., Fog water collection: Challenges beyond technology.

Water (Switzerland), vol. 10, pp. 372, 2018.

5. Zheng, Y., Bai, H., Huang, Z., Tian, X., Nie, F.Q., Zhao, Y. Zhai, J., Jiang, L., Directional water collection on wetted spider silk, *Nature*, vol. 463, pp. 640–643, 2010.
6. Uddin, M. N., Desai, F. J., Rahman, M. M. & Asmatulu, R. Highly Efficient Fog Harvester of Electrospun Permanent Superhydrophobic-Hydrophilic Polymeric Nanocomposite Fiber Mats. *Nanoscale Advances*, Nanoscale Advances, vol. 2, pp. 4627-4638, 2020.
7. Uddin, M. N., Desai, F. J. & Asmatulu, E, Biomimetic electrospun nanocomposite fibers from recycled polystyrene foams exhibiting superhydrophobicity, *Energy, Ecology and. Environment*, vol, 5, pp. 1–11, 2020.
8. Salahuddin, M., Uddin, M. N., Hwang, G. & Asmatulu, R., Superhydrophobic PAN nanofibers for gas diffusion layers of proton exchange membrane fuel cells for cathodic water management, *International Journal of Hydrogen Energy*, vol. 43, pp. 11530–11538 2018.
9. Uddin, M. N., Rahman, M. M. & Asmatulu, R. Efficient fog harvesting through electrospun superhydrophobic polyacrylonitrile nanocomposite fiber mats, in Proc. SPIE *Bioinspiration, Biomimetics, and Bioreplication X*, vol. 11374, 31, 2020.
10. Uddin, M. N., Rahman, M. M. & Asmatulu, E. Sustainable freshwater harvesting from atmosphere through nanocomposite fibers of recycled polystyrene foams, in Proc. SPIE *Behavior and Mechanics of Multifunctional Materials IX*, vol. 11377, 52, 2020.
11. Jurak, S. F., Jurak, E. F., Uddin, M. N. & Asmatulu, R., Functional superhydrophobic coating systems for possible corrosion mitigation, *International Journal of Automation Technology*, vol. 14, pp.148–158, 2020.
12. Parker, A. R. & Lawrence, C. R., Water capture by a desert beetle, *Nature*, vol. 414, pp. 33–34 2001.
13. Subeshan, B., Usta, A. & Asmatulu, R. Deicing and self-cleaning of plasma-treated superhydrophobic coatings on the surface of aluminum alloy sheets, *Surfaces and Interfaces*, vol. 18, pp. 23105, 2020.
14. Wang, Y., Zhang, L., Wu, J., Hedhili, M. N. & Wang, P., A facile strategy for the fabrication of a bioinspired hydrophilic-superhydrophobic patterned surface for highly efficient fog-harvesting, *Journal of Material Chemistry A*, vol. 3, pp. 18963–18969, 2015.
15. Azad, M. A. K., Krause, T., Danter, L., Baars, A., Koch, K. & Barthlott, W., Fog Collection on Polyethylene Terephthalate (PET) Fibers: Influence of Cross Section and Surface Structure, *Langmuir*, vol. 33, pp. 5555–5564, 2017.
16. Almasian, A., Chizari Fard, G., Mirjalili, M. & Parvinzadeh Gashti, M., Fluorinated-PAN nanofibers: Preparation, optimization, characterization and fog harvesting property, *Journal of Industrial and Engineering Chemistry*, vol. 62, pp. 146–155, 2018.
17. Asmatulu, E., Subeshan, B., Twomey, J. & Overcash, M., Increasing the lifetime of products by nanomaterial inclusions—life cycle energy implications, *International Journal of Life Cycle Assessment*, 2020. doi:10.1007/s11367-020-01794-w.
18. Lei, J. & Guo, Z., A fog-collecting surface mimicking the Namib beetle: Its water collection efficiency and influencing factors, *Nanoscale, vol.* 12, pp. 6921–6936, 2020.
19. Saufi, S. M. & Ismail, A. F., Development and characterization of polyacrylonitrile (PAN) based carbon hollow fiber membrane, *Songklanakarin Journal of Science and Technology*, vol. pp. 24, 843–854, 2002.
20. Goracheva, V. O., Mikhailova, T. K., Fedorkina, S. G., Konnova, N. F. Azarova, M. T., Konkin, A. A., Thermographic and thermogravimetric analysis of the thermal behaviour of polyacrylonitrile fibres, Fibre Chemistry, vol. 5, pp. 496–498, 1974.
21. Sas, I., Gorga, R. E., Joines, J. A. & Thoney, K. A., Literature review on superhydrophobic self-cleaning surfaces produced by electrospinning. *Journal of Polymer Science Part B: Polymer Physics, vol.* 50, pp. 824–845, 2012.
22. Alexander, T., Subeshan, B. & Asmatulu, R., Modifying the figure of merit of thermoelectric materials with inclusions of porous structures. *Energy, Ecology and Environment*, vol. 5, pp. 313–329, 2020.
23. Thickett, S. C., Neto, C. & Harris, A. T., Biomimetic surface coatings for atmospheric water capture prepared by dewetting of polymer films, *Advanced Materials*, vol. 23, pp. 3718–3722, 2011.
24. Andrews, H. G., Eccles, E. A., Schofield, W. C. E. & Badyal, J. P. S., Three-dimensional hierarchical structures for fog harvesting, *Langmuir*, vol. 27, pp. 3798–3802, 2011.
25. Lee, A., Moon, M. W., Lim, H., Kim, W. D. & Kim, H. Y., Water harvest via dewing. *Langmuir*, *vol.* 28, pp. 10183–10191, 2012.